JPP JOURNAL OF PROTEINS AND PROTEOMICS
3(2), July-December 2012, pp. 157-168

REVIEW ARTICLE

NUCLEATION AND ENTROPY COMPENSATION IN BIOLOGICAL ASSEMBLY

Frank A. Ferrone

Department of Physics, Drexel University, Philadelphia, PA 19104, USA

Abstract: The assembly of molecules from solution into larger aggregates de-activates their independent rotational and translational motion, which would represent an insuperable penalty in free energy without a compensatory mechanism for regaining at least some of the lost entropy. Such compensation is provided by the internal rigid-body motion of molecules in protein aggregates such as polymers and crystals. While the concepts behind the contributions of these entropic elements, known as vibrational entropy, are not new, the magnitude of the effects is little appreciated. Based on extensive experiments on sickle cell hemoglobin polymerization, we present examples showing the magnitude of the effects and the role they play in explaining such things as the rapid assembly of fibers compared with crystals. While the examples will be drawn from sickle hemoglobin, the principles and applications of the concepts are quite general.

Keywords: Nucleation; sickle-cell disease; self-assembly; kinetics.

Introduction

Sickle cell disease is perhaps the oldest member of an expanding class of diseases that entail pathological assembly, including such prominent maladies as Alzheimer's disease, prion diseases, and diabetes. While the more recent members of the class also involve a misfolding step, assembly remains a common element of their pathology, whether it is through large structures or small oligomers. Sickle hemoglobin aggregation does not begin with a misfolding step, but is set in motion by the small, normal quaternary structural change that accompanies the removal of oxygen (or other ligand). Because the structures of the monomeric, aggregation competent species are known, and there are reasonable models for the fibrous aggregates, the study of the assembly permits greater detail than processes where there remains uncertainty about the constituent elements. The study of hemoglobin polymer assembly has led to a quite simple yet accurate model, including, for example, the effects of molecular crowding. The nucleation process is the focus of the present treatment, since it may be applicable to other assemblies.

Hemoglobin is a tetrameric protein, with two a and two b subunits, having a mutation site on the surface of the latter in sickle hemoglobin (HbS). There, a charged group (glu) has been replaced by a hydrophobic one (val). Oxygen delivery is well known to cause a small rearrangement of the subunit packing, and the deoxygenated form brings the mutation site and a receptor pocket into register, allowing long, 14 stranded fibers (or polymers—the terms will be used interchangeably) to be formed. The reaction is reversible, and oxygen binding changes Hb structure back into one incommensurate with the fibers, dissolving polymers that have formed as well as prohibiting the formation of new ones.

Hemoglobin polymerization is now known to occur by two pathways. (Ferrone *et al.*, 1980; Ferrone *et al.*, 1985a) (Figure 1). A homogeneous

Corresponding Author: **Frank A. Ferrone**
E-mail: fferrone@drexel.edu

Received: November 9, 2012
Accepted: November 22, 2012
Published: November 30, 2012

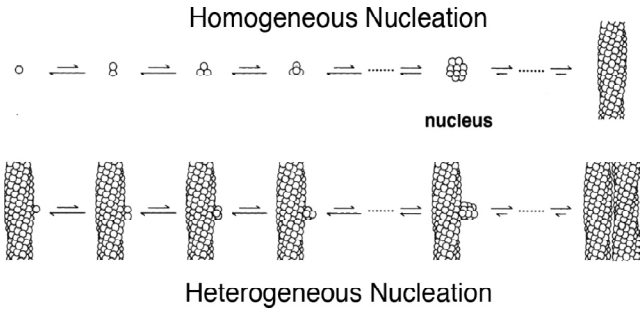

***Figure 1*. The double nucleation model for hemoglobin polymerization. In the homogeneous nucleation pathway, molecules in solution randomly assemble in a series of unfavorable steps until a reaction turning point is reached, called the nucleus. Post-nuclear steps are down-hill. In the heterogeneous nucleation pathway, nuclei can form on the surface of other polymers, formed by either pathway. Even in heterogeneous nucleation, the steps are unfavorable up to the nucleus.**

nucleation process creates the first polymers in solution, while heterogeneous nucleation generates polymers on the surface of other polymers. The heterogeneous process generates arrays of polymers, known as domains, which scatter light prolifically. This makes homogeneous nucleation much easier to detect, since the product of each nucleus is a large polymer domain. Essentially all methods for studying nucleation have taken advantage of this aspect of the process.

Experimental Methods to Measure Nucleation

Sickle hemoglobin polymerization under physiological conditions occurs in less than seconds and yet requires relatively high concentrations (>170 mg/ml). (Ross *et al.*, 1977). This created experimental challenges for initiation of the polymerization, as well as placing limitations on the types of spectroscopic methods that could be used (Sunshine *et al.*, 1979). Important early insights were nonetheless achieved by a number of studies mainly using simple temperature jump techniques (Hofrichter *et al.*, 1976).

In the 1970's a very useful method was introduced, which employed light to remove CO that was bound to Hb in place of oxygen (with similar inhibition of polymerization while it was bound) (Ferrone *et al.*, 1980; Ferrone *et al.*, 1985b). A laser could easily be focused into a small spot, and provide the requisite continuous photon flux to create and sustain a region of completely deoxygenated Hb, without any significant temperature rise. This method was subsequently employed on red cells as well (Coletta *et al.*, 1982). The photolysis method for inducing polymerization could be coupled with various detection modalities, including light scattering (Ferrone *et al.*, 1985b), birefringence (Basak *et al.*, 1988), absorbance (Cho and Ferrone, 1990), or DIC microscopy (Briehl, 1995; Galkin and Vekilov, 2004).

The simplest experiment is to follow the appearance of polymers as a function of time by observing the dramatic amount of light that they scatter. In such experiments, the simplest assumption has been to take the amount of material polymerized as proportional to the amount of light scattered. The rate equations that describe the process permit a robust way to separate the homogeneous nucleation rate. It has been shown that the concentration of polymerized monomers Δ can be described as

$$\Delta = A\,[\cosh Bt - 1] \sim A\exp Bt (Bt >> 1) \qquad (1)$$

in which A and B contain parameters of both nucleation processes (Bishop and Ferrone, 1984). For larger Bt, this curve becomes exponential, and gives the reaction an apparent delay. Typical data is shown in Figure 2. This "delay time", which is very roughly 1/B, is a convenient empirical measure of the reaction. Quantification of such a "delay" is done by extrapolation. While this is intuitive for considering the point in time when the reaction becomes explosively apparent, and begins to make substantial change in solution properties such as stiffness of a cell, it is mathematically awkward for comparing with theory. A similar measure somewhat more amenable to comparison with theory is the tenth time, viz., the time to get 1/10 of the reaction. For any detailed attempt to relate the observation to underlying behavior, though, fitting the data to get the parameters A and B is most helpful.

An important feature of the preceding mathematics that is easily overlooked is that the exponentials are taken from time 0, not from when the curves begin to grow. This is profound because it means there is no change in the processes once growth is observed: it entirely exponential. This contrasts with the oft-heard but incorrect

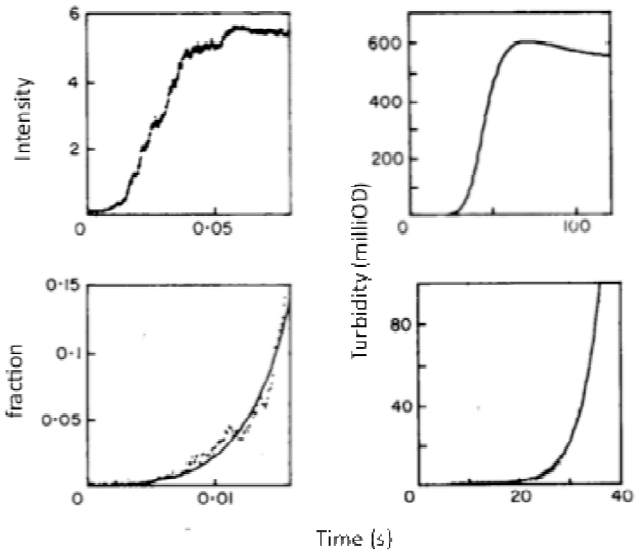

Figure 2. **Typical kinetic curves plus fits to the initial reaction. On the left (5.79 mM, 24.4 °C), photolysis has induced the reaction (see text), and light scattering of the photolysis beam is used to follow the reaction. On the right (3.95 mM, 25°C), the reaction has been induced by a sudden rise in temperature, and the reaction monitored by the resulting turbidity of the solution. In the bottom panels, equation 1 has been used to fit the data. Note that the exponential fit (in the right hand panel) begins at time = 0. Such an exponential has an apparent "delay", as can be seen, despite beginning from the origin (based on Ferrone *et al.*, 1985a).**

identification of the delay period as the time during which nuclei are being formed. This is discussed extensively elsewhere (Ferrone, 1999). A corollary of this is that, since the "delay" is observational, the use of more sensitive probes will clearly shorten the period before a signal is observed.

The use of this relationship does presuppose the proportionality of light scattering to the mass of polymerized hemoglobin. Such proportionality is plausible because, unlike the usual light scattering from polymer rods, for example, the scattering from the growing domains is always likely to be in the multiple scattering regime, and simply represents scattering from a rough but growing object. There has been no rigorous test of this, however.

Even though both A and B contain contributions from both nucleation pathways, the combination B^2A contains only homogeneous nucleation and growth; the heterogeneous process (or any secondary nucleation process, such as fragmentation) drops out. If f_o is the rate of homogeneous nucleation and J is the rate of polymer growth, then

$$B^2A = Jf_o \tag{2}$$

Therefore, the study of this product is a robust way to investigate homogeneous nucleation. (Note the convention of referring to nucleation as f_o serves to emphasize that this is the rate at the beginning of the reaction, before monomer depletion has begun to slow it). This method was used in an extensive study that used both laser photolysis and temperature jump experiments to initiate the reaction (Ferrone *et al.*, 1985b). The congruity of the results of both methods in their common regions of conditions also had the benefit of supporting the simple approximation of the proportionality of light scattering to polymer mass, since different wavelengths and geometries were used, yet similar results were obtained.

When nucleation occurs in a small enough volume, that region may be filled with polymers generated from one single homogeneous nucleus (This propertywas central to the discovery of the secondary nucleation process). Nucleus formation is a barrier crossing process and thus each nucleation event is intrinsically stochastic. When many nuclei form, their randomness is masked in the average, but when a single nucleus can be viewed, its stochastic nature is clear. Correspondingly, the collection of a distribution of tenth times provides another means of determining the nucleation rate. The probability of a given tenth time has been shown to be (Szabo, 1988).

$$T(l) = \frac{Bn^{\zeta/B}}{\Gamma(\zeta/B)}\left(1-e^{-Bt}\right)^{A} e^{-\zeta t} \tag{3}$$

ζ is the rate of homogeneous nucleation in the interrogated volume V_o, n is the number of events that are in the observation threshold, B is as defined above and Γ is a gamma function. The parameter n is typically large (10^3 to 10^6). It describes the point at which observation is made, and can be shown to be equal to $2\theta\ (c_o - c_s)N_o VB/J$ in which N_o is Avogadro's number, and J is the net rate of polymer elongation. c_o and c_s are initial concentration and solubility, respectively (Aprelev *et al.* 2005). θ is a threshold parameter, here taken as 1/10 for measurements of tenth-time. The distribution described by eqn. 3 begins small because of the $1 - e^{-Bt}$ term. Once $t > 1/B$,

the distribution becomes a decaying exponential, whose decay constant is ζ, the rate of homogeneous nucleation. The rate constant for homogeneous nucleation, f_o, measured in mM/s, is related to z by

$$\zeta = f_o N_o V_o. \quad (4)$$

where the constants N_o and V_o are described above.

This method is insensitive to light scattering linearity, since that only affects the threshold parameter *n*, while the nucleation rate is observed in the decay tail of the distribution. Typical distributions are shown in Fig. 3. The distribution lacks small tenth times because objects less than the critical size *n* are invisible, and thus they must grow to a minimal size to be seen. The observation of the stochastic variation was first used by repeatedly photolyzing the same spot (Ferrone *et al.*, 1985b; Hofrichter, 1986). Subsequently, a parallel detection method was developed that facilitated collection of large amounts of data (Cao and Ferrone, 1996, 1997), as well as allowing intrinsic controls for experiments with cell membranes, for example (Aprelev *et al.*, 2005).

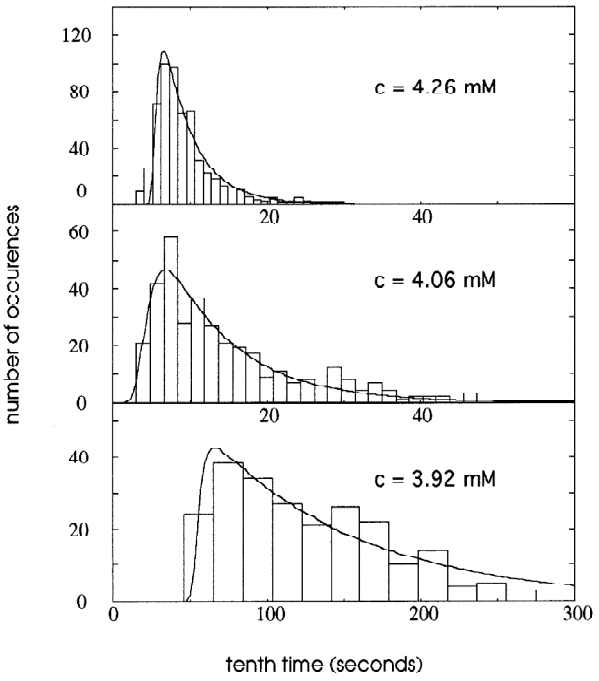

***Figure 3*. Stochastic variation of tenth times for polymerization. When a volume that contains only a single nucleus is viewed, the onset times (e.g. tenth time) display stochastic variation, due to the randomness inherent in the crossing of the nucleation barrier. Experiments were conducted in parallel photolysis methods to allow consistent collection of large amounts of data. Note the variation of times as concentration is changed, which is the result of the nucleation process coupled with large activity coefficients. The solid curves are the fits of eqn. 3 (based on Cao and Ferrone, 1996).**

The foregoing method yields nucleation rates by using light scattering to sense the formation of domains and equating domain number to the number of nuclei. It is also possible to observe the number of domains by DIC microscopy which uses diffraction shadows to visualize the wispy 20 nm diameter fibers and their clustering in domains in the types of images seen in Figure 4 (Galkin and Vekilov, 2004; Galkin *et al.*, 2007).

This data can be analyzed from the perspective of Szabo's distribution function as well. For illustrative purposes, a simplified form of the Szabo distribution will be used (Hofrichter, 1986). This fully suppresses short time values by assuming that up till some critical time τ (normally close to the delay time), nothing happens, whereas afterwards the probability of finding a nucleation event falls as exp (-ζt). Following normalization, this distribution looks like

$$T(t) = \zeta \exp(-\zeta(t - \tau)) \quad (5)$$

In the studies using this DIC method, the net probability (equivalent to the net number of domains) has been evaluated rather than the distribution. Integrating the simpler equation gives

$$N(t) = \int_0^t T(t')dt' = 1 - \exp(-\zeta(t - \tau)) \quad (6)$$

When the argument of the exponent is small, the net number of domains is simply

$$N(t) \sim \zeta(t\text{–}t) \quad (7)$$

which corresponds well with the observations, as seen in Figure 4. For the original class of experiments, such as those of Hofrichter (1986), the time τ is essentially the usual Hb-observed delay time. For DIC experiments, the first observations are made much earlier. The delay τ is still the result of observational limits, as expressed in the Szabo formulation, rather than a time required to establish the equilibrium distribution (e.g. (Galkin and Vekilov, 2004; Galkin *et al.*, 2007)). (The reader should also be aware that the term "delay time" as described by

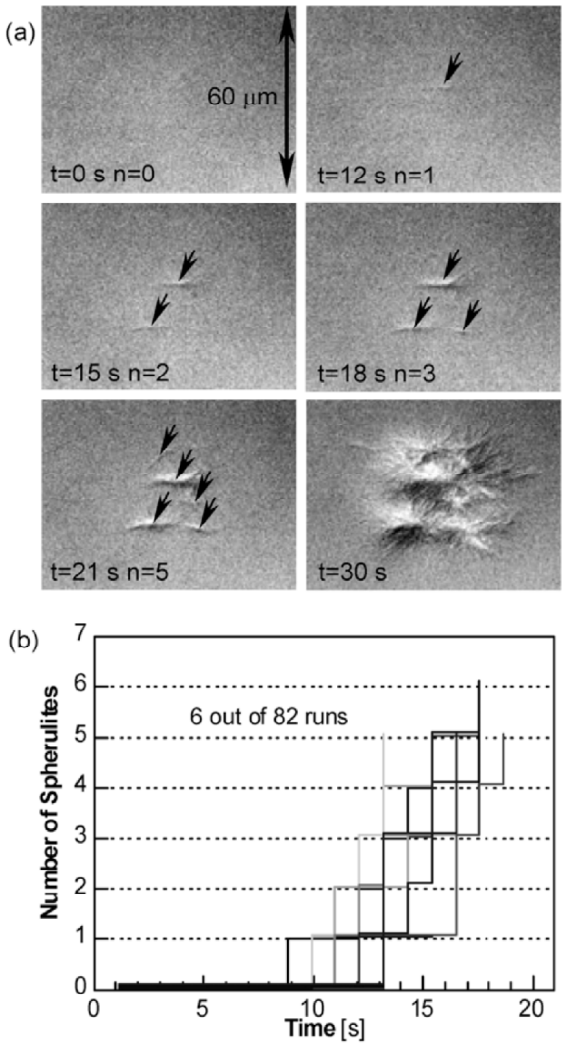

Figure 4. **Growth of polymer domains by photolysis, viewed in DIC microscopy. (22 °C and3.6 mM) Domains nucleate from a single homogeneous nucleation event, so that counting domains is equivalent to enumerating nucleation events. The bottom panel shows the number of domains as a function of time for six replications. The linearity as well as delay is predicted by eqn 7, which is essentially the same relationship that fit the data in Fig. 3 (based on Galkin and Vekilov, 2002).**

those particular authors refers to a very different concept, viz. the time required to establish an equilibrium distribution of species in nucleation kinetics, despite the similar nomenclature. That set-up time has been taken as sufficiently short to be neglected in the treatments described here).

In multidomain experiments, a potential complication arises from the consumption of monomers by adjacent domains. Since nucleation rates are highly concentration dependent, lowering monomer concentrations can have the effect of suppressing rates in the domains formed later in the observation. For photolysis experiments, this is offset to a great degree by a large reservoir of monomers outside the photolyzed area that will diffuse into the illuminated region as its monomers are depleted (Cho and Ferrone, 1991; Cho and Ferrone, 1990). This serves to mitigate somewhat the effect of monomer consumption. One further concern is that once a domain is formed, its volume is no longer available to further nucleation. This makes the first domain formation times more reliable, though as shown above, strict linearity would only apply in the small ζt limit anyway.

Birefringence may also be used to count the number of domains, and so infer the number of nuclei (Christoph *et al.*, 2005). Such an experiment is shown in Figure 5. This is clearly a time independent version of the previous experiment. This approach has the virtue of requiring the simplest apparatus, viz. a polarizing microcroscope, and does not require laser photolysis. However, it is likely to undercount the absolute number of domains for three reasons. First, as discussed above, the available volume diminishes as domains are formed. Secondly, as the earliest-formed domains consume monomers there is no longer a virtually endless reservoir to restock the solution phase, so the monomer concentration inevitably decreases. Finally, spherulites are actually a later evolution of polymer domain morphology, as shown in experiments as well as simulations (Basak *et al.*, 1988; Dou and Ferrone, 1993) (Figure 4 for example clearly shows domains that are far from spherulitic). The method therefore is better suited for measuring concentration or temperature dependence, rather than measuring absolute rates.

A composite graph of data collected at 25°C for all the above methods is shown in Figure 6. Because of the problems that are intrinsic to the counting of polymer domains (as recognized by the authors themselves), the data of Christoph *et al.* (2005) was adjusted by a single common factor to match the other data sets. All the remaining data was used as published. The combination of the various methods have spanned 11 orders of magnitude of rates of homogeneous nucleation, providing a fertile

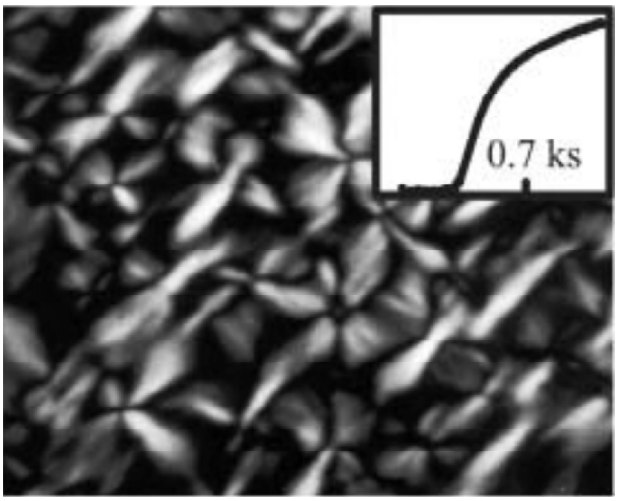

Figure 5. **Polymer domains viewed between crossed polarizers. The alignment of polymers in roughly spherulitic form in the domains yields a birefringence that can be viewed as shown. The time dependence of the net birefringence is shown in the inset. As in Figure 4, each domain is the consequence of a homogeneous nucleation event. However, the mutual occlusion of space causes the absolute number of domains to be undercounted, though the variation with conditions appears accurate. The sample shown had 3.98 mM Hb, polymerized at 30°C (based on Christoph *et al.*, 2005).**

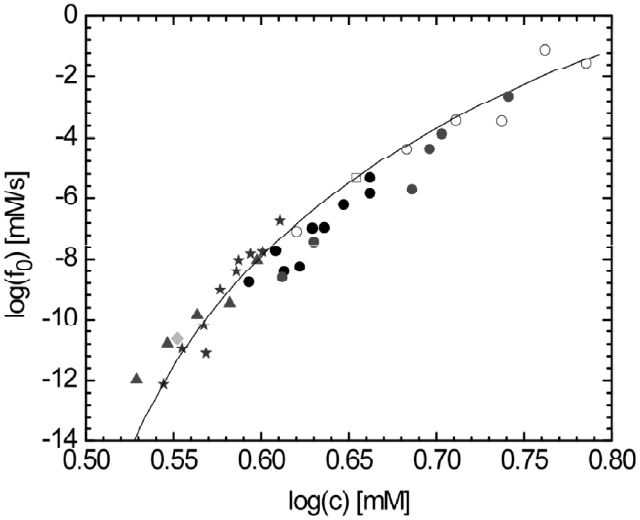

Figure 6. **Log-$_{10}$ of homogeneous nucleation rate as a function of log$_{10}$ of initial concentration, at 25°C. Open circles are photolysis data from Ferrone *et al.*, 1985a. Filled triangles are temperature jump data from the same source. Stars are data from Christoph et al (2005), adjusted vertically (all by the same amount) to best match the theory curve. The open square is taken from Hofrichter (1986) measured by stochastic variation. Dark filled circles are also measured by stochastic variation, taken from Cao and Ferrone (1996) and from Ivanova *et al.* (Ivanova *et al.*, 2000). Lighter filled circles (red) are measured by stochastic variation, from data of Aprelev, Rotter, Zakharov and Ferrone (unpublished). The diamond is domain growth data of Galkin and Vekilov (2002). The curve is the fit of the simple nucleation theory (eqn. 13) described in the text.**

proving ground for nucleation theory, to which we turn next.

Theory

The power of nucleation rate measurements to reveal underlying behavior arises because the rate of homogeneous nucleation is proportional to the activity of the nuclei, that is, the concentration of nuclei times an activity coefficient. Thus the study of nucleation kinetics can reveal the concentration of the small nuclear clusters. Mathematically, one may write

$$f_0 = k_+ \frac{\gamma_0 C_0 \gamma_{i^*} C_{i^*}}{\gamma^\ddagger} \qquad (8)$$

The term in the denominator, gamma dagger, is an activated complex activity coefficient, where the activated complex is taken as the nucleus plus one monomer (i.e. i^*+1) (Ferrone *et al.*, 1985a). The other gammas likewise represent the specific activity coefficients. The theory and experiment converge in the specification of concentration (or activity) of the nuclei.

This formulation assumes that when a nucleus crosses the nucleation barrier, its traversal is irreversible. Thus the nucleation equations typically contain no "back rate" terms, though a correction known as the Zeldovich factor, based on the curvature of the free energy surface, is often used for this purpose (Abraham, 1974).

The simple nucleation theory used has been described previously (Ferrone, 2006), and so will only be sketched here. The theory derives an expression for the concentration of nuclei by equating the chemical potential of the monomers and that of the aggregates. Two key concepts underlie the calculation. The first is that the nucleus involves no special structure, but simply represents a small piece of the infinite polymer. This allows the intermolecular contacts to be equated to those that are also found in the equilibrium, long and essentially infinite polymers. The second concept is that the structures are at equilibrium, so that their concentration may be derived from their free energy, which in turn may be determined from the various constituent chemical potentials. These are: (1) μ_{TR} the chemical potential of the monomer

free in solution, which has translational and rotational entropy; (2) μ_{PC}, the chemical potential of the monomer contacts or "bonds" within the polymer and (3) μ_{PV}, the chemical potential that arises from center of mass vibration of the monomers within the polymer. These all combine to give the solubility c_s, e.g.

$$RT \ln \gamma_s c_s = \mu_{PC} + \mu_{PV} - \mu_{TR} \quad (9)$$

The same principle is involved in forming aggregates. The monomers lose entropy of rotation and translation in the solution. Once assembled into an aggregate, they gain energy based on the intermolecular contacts that are formed. Such a model of the nucleus requires that its structure be known, so as to have a reliable way of estimating contacts between molecules for different sized aggregates. The approach taken heretofore has been to treat all contacts as equivalent, and in so doing, to employ a previously published calculation of the number of contacts between hard spheres in random association (Ginnel, 1961). This calculation of contact numbers was a numerical result that could be approximated by an analytic function that had the virtue of also giving an analytic solution for the nucleus size. Thus $\delta(n)$, the fraction of contacts made for a given size n was written as

$$\delta(n) = 1 - \delta_1 \frac{\ln n}{n} - \delta_2 \frac{1}{n} \quad (10)$$

The nucleation rate that is solved, however, contains the product $\delta_1 \mu_{PC}$. It is related to the local slope of the free energy cost. The formulation allows for a simple expression of the nucleus size, for example. It is useful to introduce an additional variable ξ, defined as

$$\xi = -(4 + \delta_1 \mu_{PC}/RT) \quad (11)$$

This leads to a nucleus expression that is particularly concise,

$$i^* = \xi / \ln S \quad (12)$$

S is defined as $\gamma c / \gamma_s c_s$ where is the solubility, and γ_s is the activity coefficient of the monomer at solubility.

It is easily shown that

$$\ln \gamma_{i^*} c_{i^*} = \xi \ln(\ln S) + \xi - \xi \ln \xi - \ln v\rho + ((1-\xi_2)\mu_{PC} + \mu_{PV}) / RT \quad (13)$$

from which the nucleation rate may be determined using eqn. 8. Only the first term varies with concentration; the remaining terms are constants. v is the specific volume of the monomer; r is the relative density of polymer to monomer. S is the major driving term being the supersaturation, but contains known quantities. The single variable is thus ξ, which allows identification of the contact energy μ_{PC}.

What is interesting about this approach is that, were a more structurally nuanced contact function $\delta(n)$ to become known (with, say, inequivalence between contact points), it would not invalidate the overall fit, but merely involve reinterpretation of parameters. Vibrational entropy here refers to the motion of the Hb molecules about their center of mass once they are within the aggregate. While this could also include changes in internal motion within the molecules themselves, as might occur in amyloid assembly for example, where there is a major structural change upon association, such motion internal to the Hb molecules has not been included here. Vibrational entropy will chiefly depend on the total number of molecules in the aggregate, and more weakly on the number of contacts between them. This is based on the notion that the vibrational contribution depends most strongly on the number of modes, which is linearly dependent on the number of molecules. In physical terms this means that it is not only the depth of the potential well but also its shape that determines the contributions to stability (cf. Figure 7).

In some treatments nucleation, one considers a free energy change that is linear in the number of molecules and an "excess free energy" of the aggregate. In the language here, the "excess free energy" term is due to the fact that the number of contacts differs from the number of molecules in the 3 dimension aggregates considered, as signified by eqn 10.

The description given above differs in form from conventional means of describing nucleation. Such approaches traditionally distinguish a bulk energy and a surface energy, or surface tension. Such an approach is quite reasonable for nucleation of liquid droplets from

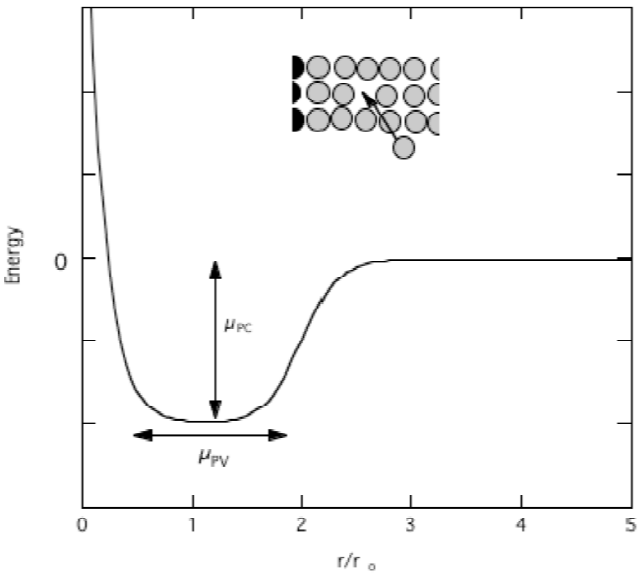

Figure 7. **Schematic potential energy well for a molecule within a polymeric aggregate. The contact energy μ_{PC} corresponds to the depth of the potential well. The vibrational chemical potential, μ_{PV} corresponds to the width of the potential well. The *x*-axis schematically shows the displacement of the molecule from r_o, its average position in the aggregate. In an aggregate, each of 6 degrees of freedom would have a well, describing the various linear and rotational motions.**

a gas, since the surface tension of the liquid phase would be known (albeit for curvatures for less extreme than that of small droplets). For crystallization, it is harder to see how to determine the surface tension of a crystallite. Most challenging to such an approach, however, is its applicability to nucleus sizes in range of 5 or so, which appears to be a nucleus size common in sickle cell polymerization: how might one distinguish surface from volume terms in such a case?

The data from the various methods in Figure 6 has been fit with the simple model above. The only parameter that gets adjusted in such a fit is the parameter x (i.e. the contact energy per eqn 11). As can be seen, almost 12 orders of magnitude of data are described by this rather simple theory.

It is also evident that the theory does not perfectly describe the data, which moreover is gathered from a variety of methods as recounted above. Certainly, the assumption that vibrational entropy solely depends on the number of molecules is oversimplified. Additionally, it is assumed (largely for lack of data) that all molecular contacts are equivalent, which also is likely to be more simple than the reality of the assembly. Likewise, the lack of a Zeldovich factor is a weakness embedded in the very beginning (viz. eqn. 8). Future developments will need to expand the theoretical developments in these directions.

Activity Coefficients and Crowding

An important feature in the theory is the presence of molecular crowding. The high concentrations at which sickle hemoglobin assembles necessitate large corrections for molecular crowding. Fortunately, Hb behaves like a hard sphere, and the nuclei can be similarly modeled, so that the rich literature available on such hard sphere interactions can be brought to bear on the problem, particularly various scaled particle theories. It turns out that the effects of crowding do not require further adjustable parameters, but can be accurately incorporated with a priori formulations (Ferrone and Rotter, 2004). As figure 8 shows, the addition of 30% or 50% crowding agent, in this case Hb—which cannot polymerize but does have the same volume as HbS— has an enormous effect on the nucleation rates. Physiologically, this effect is seen in the presence of hemoglobins such as HbF or HbA, which do not polymerize but do take up space (Rotter *et al.*, 2005; Rotter *et al.*, 2011). Even in the case of hybridization, such as with HbA, where polymerization of the hybrids is possible, the corrections are essential to analysis of the data.

The Importance of Vibrational Entropy

From the data presented one can develop a picture of the nucleation process including a balance sheet. As shown in eqn 12, one of the interesting features of the model presented is that the nucleus size will vary with concentration. Over the range shown here the nucleus size goes from 2.8 at 6.2mM, to 17.6 at 3.4mM. At typical intracellular concentrations (5mM), the nucleus size is 5.

The energetic balance reveals a remarkable cancellation, as seen in Table I (Cao and Ferrone, 1997). The large surrender of free energy due the loss of rotation and translational motion of the

Table I
Free Energies in Sickle Hemoglobin Polymerization* (kcal/mol) (25°C)

Overall Free Energy (solubility)	–1.5
Solution Rotational and Translational Energy	–35.5
Contact Energy	–7.5
Vibrational Energy in Polymer	–26.5

*Based on Cao and Ferrone (1997)Figure Legends

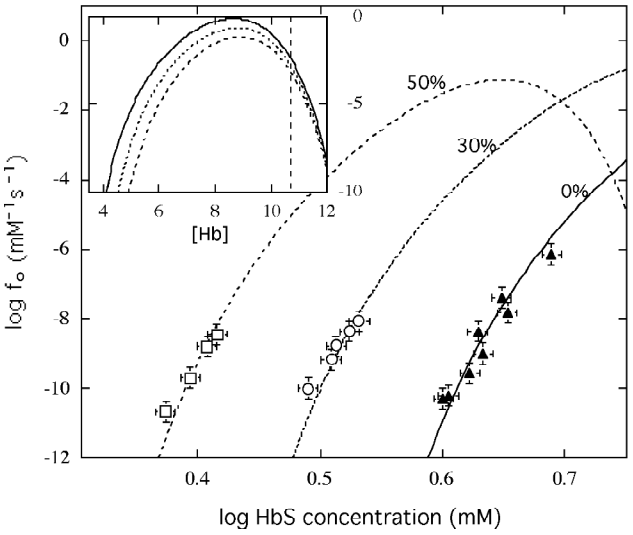

Figure 8. **Homogeneous nucleation rates at 25°C as a function of HbS concentration for various degrees of crowding. Data is from Ivanova *et al.* (2000). The abscissa shows the common log of initial HbS concentration. As cross-linked HbA is added to increase crowding, the rate of nucleation increases dramatically. 0%, 30% and 50% crowders are shown. The lines show the theoretical predictions from scaled particle theory and the thermodynamic treatment of nucleation which give an excellent description of the data with no further adjustable parameters. The inset shows the log of nucleation rates vs. total millimolar Hb concentration (on a linear scale) over enough of a range to clearly demonstrate the existence of a maximum. The dashed vertical line is the concentration of hemoglobin in polymers, and thus represents a physical upper limit to the density of the solution. Because total concentration is shown in the inset, the sequence of 0%, 30% and 50% crowding is reversed relative to the main figure. The maximum occurs because activity coefficients for the activated complex overtake the activity of the nucleus (cf. eqn. 8) as concentration becomes high enough.**

monomers in solution would be difficult to recover were it not for the motion of the molecules within the aggregated polymeric structure, which dwarfs the intermolecular contact energy. In molecular terms, the entropy of the motion within the aggregates is the consequence of the shape of the potential well in which the monomers vibrate: a shallower well allows greater movement and more entropy. The macroscopic manifestation of this broad potential minimum is the ability of the polymers to flex. This contrasts with crystals, in which the intermolecular potentials create a far more rigid environment. Vibrational entropy is thus a manifestation of an effective intermolecular potential that enables polymers to distort more readily than crystals as well as to nucleate more rapidly than crystals.

The foregoing assertion received dramatic supportfrom nucleation measurements in the double mutant, HbC-Harlem (Ivanova *et al.*, 2001), which has as a mutation in the receptor pocket in addition to the sickle mutation. The receptor mutation creates a hydrogen bond, with the readily observed consequence that crystals form instead of polymers. Perhaps most remarkable, the nucleation rate of the crystals drops by 11 orders of magnitude. The crystals appear to have essentially the same solubility as the polymers. Analysis of the nucleation rate of the crystals implied that their contact energy was significantly greater than that found in the polymers, in agreement with the known change in the contact region. With no change in the solubility, the stronger contact energy had come at the expense of the vibrational chemical potential (recall eqn. 9). The way this works is that, in compensation for the loss of entropy of removing molecules from solution, the vibrational compensation comes into play before the energetic compensation based on the number of *contacts* in the aggregate.

This difference in rates between HbS nucleation and crystal nucleation has been noted elsewhere (Galkin and Vekilov, 2004; Galkin *et al.*, 2007). From the foregoing discussion, the explanation appears to be simply that the rigidity of the crystals suppresses a vibrational entropy contribution that allows the rapid nucleation of flexible fibers.

Liquid-Liquid Demixing

The formation of ordered polymeric aggregates from isolated protein molecules resembles the condensation of a gas into a solid phase, presenting the clear question of the existence of a liquid phase as well. Such a liquid phase would be a dense protein aggregate without long-range or long-time structure. Because this protein liquid

would emerge from proteins already dissolved in solvent, the process is also described as one of liquid-liquid demixing (LLD), i.e. the spontaneous separation of the protein solution into dense protein regions and protein-depleted regions of solvent. Such a mechanism was intriguing because simulations had shown that crystallization rates could be enhanced when the conditions were near aspinodal line, which separates nucleated LLD from down-hill (non-nucleated) LLD (ten Wolde and Frenkel, 1997). The former, thanks to a nucleation barrier, represents a metastable phase, while the latter clearly is an unstable phase. Adding to the plausibility of this demixing was the increase of light scattering that one would expect from critical fluctuations below the spinodal (San Biagio and Palma, 1991; Vaiana *et al.*, 2005; Manno *et al.*, 2004). Moreover, when the fluctuations were interpreted as signifying a spinodal temperature T_s, the polymerization could be scaled onto a universal curve based on the difference of the temperature T from the spinodal T_s (Vaiana *et al.*, 2003). A two-step theory for such processes has accordingly been presented (Kashchiev *et al.*, 2005). The hypothesis of LLD was reinforced by the observation of droplet-like entities in DIC imaging (Galkin *et al.*, 2002).

A critical review of the evidence in support of LLD suggests that all the associated phenomena appear to be suitably explained at the time of this review by other means that do not require the LLD hypothesis. Consider first the "critical fluctuations". The presence of small aggregates will also sharply increase with temperature (and so will scattering) simply due to the enthalpy of their formation. Let the concentration of the scattering aggregate be denoted c_n. Then

$$\gamma_n c_n = K(\gamma c)^n = e^{\ln K}(\gamma c)^n \tag{14}$$

ln *K* may be expanded around a reference temperature T_o, viz.

$$\ln K(T) = \ln K(T_o) + \left(\frac{d\ln K}{dT}\right)_{T_0} \delta T \tag{15}$$

where δT could be the temperature in °C. Further, $(d \ln K/dT) = \Delta H/RT^2 \equiv b$. Defining $a \equiv \left(K_o(\gamma c)^n / \gamma_n\right)$ it follows that

$$c_n = a\, e^{b\delta T} \tag{16}$$

which shows a clear, sharp rise as temperature is changed. While critical fluctuations will diverge at a spinodal temperature, and so show a different functional dependence than exponential, the actual data is insufficient to distinguish the two cases (Wang and Ferrone, in preparation). Moreover, the presence of small aggregates is inevitable, thanks to the attraction that draws the molecules into a polymer, so that the only question is the magnitude of the enthalpy involved. We have found this enthalpy to be comparable to that already known for aggregation of HbS (Wang and Ferrone, in preparation).

Using the above formulation, one can reinterpret the "spinodal" temperatures. These are determined by using the reciprocal of light scattering and extrapolating to where the reciprocal intensity is zero. If the intensity of scattered light is given as $I = I_o + I^* e^{b\delta T}$ then the "spinodal temperature" δT_s can be shown to be

$$\delta T_s = \frac{1}{b}\left(\frac{I_o}{I^*} - 1\right) = \frac{T_o^2}{^2H}\left(\frac{I_o}{I^*} - 1\right) \tag{17}$$

Since I^* contains the constant a above, which in turn is a stronger function of c than is I_o, this temperature will decrease as concentration increases.

It has also been argued that spinodal temperatures and nucleation are linked because the nucleation kinetics can be scaled when the actual temperatures are related to the spinodal temperatures. However, a simple Taylor expansion of the nucleation rate about the spinodal gives the same result:

$$\begin{aligned} \ln f_o(T) &= \ln f_o(T_s) + \frac{\partial \ln f_o}{\partial T}\left(T - T_s\right) \\ &= \ln f_o(T_s) - \frac{\xi}{T_s^2 \ln S(T_s)}\Delta H \cdot (T - T_s) \\ &= \ln f_o(T_s) - \frac{\xi}{\ln S(T_s)}\left(\frac{T_o}{T_s}\right)^2\left(\frac{I_o}{I^*} - 1\right)\left(\frac{T - T_s}{T_s}\right) \end{aligned} \tag{18}$$

where the second equality arises because ξ is essentially temperature independent (Cao and Ferrone, 1997) and the third equality comes from

substituting the spinodal temperature from the above equation. The quantity $(T - T_s)/T_s$ is the reduced temperature, referred to as ε elsewhere (Vaiana *et al.*, 2003).

Not only can the observed scaling be explained, but there are also problems that arise were one to interpret the nucleation process as driven by LLD. The formation of the dense liquid at temperatures above the spinodal is, by definition, the demixing of an unstable phase, and so, lacking a nucleation step, will have minimal concentration dependence. (The only reason to have any concentration dependence greater than unity is the presence of activity coefficients). Once the dense protein liquid forms, with minimal concentration dependence, its transformation into an ordered dense structure from a disordered one is an isomerization reaction (in that the reactants are changing position, not engaging in an association), and that, in turn, has no concentration dependence. The upshot is that, for demixing to power the protein assembly process, it would have a concentration dependence well below that which is observed experimentally. Consider the following example. Vaiana *et al.* (2003) showed scaling for the exponential growth rate *B*, which was experimentally determined to have ~ 10^{th} power concentration dependence (at 4.65 mM and 35 °C) (Ferrone *et al.*, 1985b). Were it driven by down-hilldemixing, it should have no greater than ~5^{th} order dependence, well outside the experimental error of the data.

Finally we turn to the observation of liquid droplets. While this was a dramatic demonstration of a demixing process, this was only observed with the additive PEG present (Galkin *et al.*, 2002). This is then a ternary solution, with the potential of a complex phase diagram including PEG-rich phases. The process is clearly interesting and exciting, but the lack of droplets without PEG makes it difficulty to argue for the LLD process as a catalyst in nucleation.

In short, the bulk of arguments that have been advanced in its support are not unique to that mechanism, and that the presence of the mechanism remains to be demonstrated as a necessary correction to the simple nucleation theory that has worked so well.

Acknowledgement

This work has been supported by the National Institutes of Health, through the National Heart, Lung, and Blood Institute. The author thanks Dr. Yi-Hua Wang for his help in preparing Figure 6.

References

Abraham, F. F. (1974). Homogeneous Nucleation Theory. Academic Press, New York.

Aprelev, A., Rotter, M.A., Etzion, Z., Bookchin, R.M., Briehl, R.W. and Ferrone, F.A. (2005). The effects of erythrocyte membranes on the nucleation of sickle hemoglobin. Biophys. J. *88*, 2815-2822.

Basak, S., Ferrone, F.A. and Wang, J.T. (1988). Kinetics of Domain Formation by Sickle hemoglobin Polymers. Biophys. J. *54*, 829-843.

Bishop, M.F. and Ferrone, F.A. (1984). Kinetics of nucleation controlled polymerization: a perturbation treatment for use with a secondary pathway. Biophys. J. *46*,631-644.

Briehl, R. (1995). Nucleation, Fiber Growth and Melting, and Domain Formation and Structure in Sickle Cell Hemoglobin Gels. J. Mol. Biol. *245*, 710-723.

Cao, Z. and Ferrone, F.A. (1996). A 50th order reaction predicted and observed for sickle hemoglobin nucleation. J. Mol. Biol. *256*, 219-222.

Cao, Z. and Ferrone, F.A. (1997). Homogeneous Nucleation in Sickle Hemoglobin. Stochastic Measurements with a Parallel Method. Biophys. J. *72*,343-372.

Cho, M.R. and Ferrone, F.A. (1990). Monomer diffusion into polymer domains in sickle hemoglobin. Biophys. J. *58*, 1067-1073.

Cho, M.R. and Ferrone, F.A. (1991). Monomer diffusion and polymer alignment in domains of sickle hemoglobin. Biophys. J. *63*, 205-214.

Christoph, G.W., Hofrichter, J. and Eaton, W.A. (2005). Understanding the shape of sickled red cells. Biophys. J. *88*, 1371-1376.

Coletta, M., Hofrichter, J., Ferrone, F.A. and Eaton, W.A. (1982). Kinetics of sickle haemoglobin polymerization in single red cells. Nature. *300*,194-197

Dou, Q. and Ferrone, F.A. (1993). Simulated Formation of Polymer Domains in Sickle Hemoglobin. Biophys. J. *65*, 2068-2077.

Ferrone, F. (1999). Analysis of protein aggregation kinetics. Methods. Enzymol. *309*, 256-274.

Ferrone, F.A. (2006). Nucleation: the connections between equilibrium and kinetic behavior. Methods. Enzymol. *412*, 285-299.

Ferrone F.A., Hofrichter, J. and Eaton W.A. (1985a). Kinetics of sickle hemoglobin polymerization II: a double nucleation mechanism. J. Mol. Biol. *183*, 611-631.

Ferrone, F.A., Hofrichter, J. and Eaton W.A. (1985b). Kinetics of sickle hemoglobin polymerization I: studies using temperature-jump and laser photolysis techniques. J. Mol. Biol. *183*,591-610.

Ferrone, F.A., Hofrichter, J., Sunshine, H. and Eaton, W.A. (1980). Kinetic studies on photolysis-induced gelation of sickle cell hemoglobin suggest a new mechanism. Biophys. J. *32*, 361-377.

Ferrone, F.A. and Rotter, M.A. (2004). Crowding and the polymerization of sickle hemoglobin. J. Mol. Recognition. *17,* 497-504.

Galkin, O., Chen, K., Nagel, R.L., Hirsch, R.E. and Vekilov, P.G. (2002). Liquid-liquid separation in solutions of normal and sickle cell hemoglobin. Proc. Natl. Acad. Sci. USA. *99,* 8479-8483.

Galkin, O., Nagel, R.L. and Vekilov, P.G. (2007). The kinetics of nucleation and growth of sickle cell hemoglobin fibers. J. Mol. Biol. *365,* 425-439.

Galkin, O. and Vekilov, P.G. (2004). Mechanisms of homogeneous nucleation of polymers of sickle cell anemia hemoglobin in deoxy state. J. Mol. Biol. *336*, 43-59.

Ginnel, R. (1961). Geometric Basis of Phase Change. J. Chem. Phys. *34*, 992-998.

Hofrichter, J. (1986). Kinetics of Sickle Hemoglobin Polymerization III. Nucleation rates determined from stochastic fluctuations in polymerization progress curves. J. Mol. Biol. *189*, 553-571

Hofrichter, J., Ross P.D. and Eaton W.A. (1976). Supersaturation in sickle cell hemoglobin solutions. Proc. Nat. Acad. Sci. USA. *73*, 3035-3039.

Ivanova, M., Jasuja, R., Krasnosselskaia, L., Josephs, R., Wang Z., Ding M., Horiuchi K., Adachi K. and Ferrone F.A. (2001). Felxibility and Nucleation in Sickle Hemoglobin. J. Mol. Biol. *314*, 851-861.

Ivanova, M., Jasuja, R., Kwong, S., Briehl, R.W. and Ferrone, F.A. (2000). Nonideality and the Nucleation of Sickle Hemoglobin. Biophys. J. *79*, 1016-1022.

Kashchiev, D., Vekilov, P.G. and Kolomeisky, A.B. (2005). Kinetics of two-step nucleation of crystals. J. Chem. Phys. *122*, 244706. doi:10.1063/1.1943389.

Manno, M., San Biagio, P.L. and Palma, M.U. (2004). The role of pH on instability and aggregation of sickle hemoglobin solutions. Proteins. *55,* 169-176.

Ross, P.D., Hofrichter, J. and Eaton, W.A. (1977). Thermodynamics of gelation of sickle cell deoxyhemoglobin. J. Mol. Biol. *115,* 111-134.

Rotter, M., Aprelev, A., Adachi, K. and Ferrone F.A. (2005). Molecular crowding limits the role of fetal hemoglobin in therapy for sickle cell disease. J. Mol. Biol. *347*, 1015-1023.

Rotter, M., Yosmanovich, D., Briehl, R.W., Kwong, S. and Ferrone F.A. (2011). Nucleation of sickle hemoglobin mixed with hemoglobin a: experimental and theoretical studies of hybrid-forming mixtures. Biophys. J. *101* , 2790-2797.

San Biagio, P.L. and Palma, M.U. (1991). Spinodal lines and Flory-Huggins free-energies for solutions of human hemoglobins HbS and HbA. Biophys. J. *60*, 508-512.

Sunshine, H.R., Ferrone, F.A., Hofrichter J. and Eaton W.A. (1979). Gelation assays and the evaluation of therapeutic inhibitors. In: Rosa J., Beuzard Y., Hercules J. (eds) Development of Therapeutic Agents for Sickle Cell Disease, vol 9. INSERM SYMPOSIUM. Elsevier-North Holland, New York, pp 31-46.

Szabo, A. (1988). Fluctuations in the polymerization of sickle hemoglobin: a simple analytical model. J. Mol. Biol. *199,* 539-542.

ten Wolde, P.R. and Frenkel D. (1997). Enhancement of protein crystal nucleation by critical density fluctuations. Science. 277, 1975-1978.

Vaiana, S.M., Palma-Vittorelli, M.B. and Palma, M.U. (2003). Time scale of protein aggregation dictated by liquid-liquid demixing. Proteins. *51*, 147-153.

Vaiana, S.M., Rotter, M.A., Emanuele A., Ferrone F.A. and Palma-Vittorelli M.B. (2005). Effect of T-R conformational change on sickle-cell hemoglobin interactions and aggregation. Proteins. *58*, 426-438.